THE AMERICAN MINERALOGIST, VOL. 53, SEPTEMBER–OCTOBER, 1968

AUTHIGENIC ALBITE FROM RHODES[1]

M. KASTNER AND D. R. WALDBAUM, *Department of Geological Sciences, Harvard University, Cambridge, Massachusetts.*

ABSTRACT

Authigenic albite crystals in Eocene limestone from Rhodes contain an hourglass structure formed by inclusions of calcite, quartz, and carbonaceous material. No detrital feldspar core is visible in the crystals. They form contact twins of two individuals after the Albite law and penetration twins of two individuals after the X-Carlsbad law. Both twin types contain the hourglass structure. Lattice parameters of the albite are: $a=8.1380$ Å, $b=12.7881$ Å, $c=7.1571$ =Å, $\alpha=94.229°$, $\beta=116.605°$, $\gamma=87.807°$. Both optical and lattice parameters indicate that the Al-Si distribution in the albite is highly ordered, although not as ordered as low albites from pegmatites and low-grade metamorphic rocks. The albite itself contains no detectable Ca or K. Lattice parameters of the calcite matrix indicate that it contains less than 1.5 mole percent $MgCO_3$ in solution.

INTRODUCTION

Authigenic feldspars are different in many respects from igneous and metamorphic feldspars. The most striking differences are their euhedral habits, unusual twins, and high chemical purity. Of particular interest are Baskin's (1956) observations that the cell dimensions of authigenic albites are substantially smaller than those of low albites from other geological environments, and the results of Füchtbauer (1950) and others which indicate relatively high optic axial angles in authigenic albites.

Albite-bearing limestones of Eocene age from the Greek island of Rhodes in the Aegean Sea, first described by Von Foullon (1891), were collected from several localities between the village of Asklipio and Yannadi Bay (36.047°N, 56.943°E) in late 1966. These are the youngest sedimentary rocks known to contain authigenic albites having no visible detrital cores, and one of the few occurrences in which the matrix rock contains little or no magnesium. In this paper we report the petrographic and crystallographic results of a preliminary investigation of this material.

LITHOLOGY

The carbonate rock in which the Rhodian albites occur is a medium dark gray (Munsell N4,[2]) micritic limestone which shows no evidence of recrystallization. The rocks, however, are structurally deformed on an outcrop scale, and the albite crystals are cut by two generations of calcite veins and these are cut subsequently by stylolites, as shown in

[1] Published under the auspices of the Committee on Experimental Geology and Geophysics at Harvard University.

[2] Geological Society of America (1963) *Rock Color Chart.*

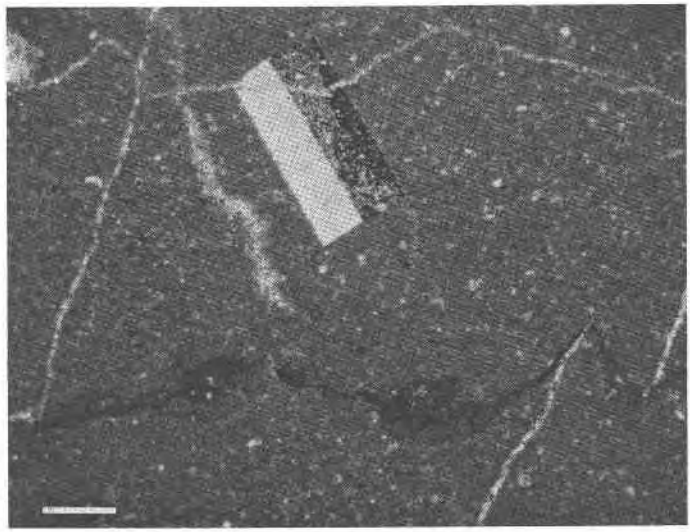

FIG. 1. Photomicrograph of albite crystals elongated parallel to (010) in micritic limestone matrix (crossed polars). Note cross-cutting relations among albite, calcite veins (white), and stylolite (black). Thin section M351; Rhodes, Greece. White line in lower left corner represents 0.5 mm.

Figure 1. No albites were found in or related to the calcite veins. This evidence indicates that the albites crystallized in one of the earliest stages of post-depositional alteration of the carbonate sediment.

Approximately 3.5 weight percent insoluble residue was extracted by dissolving the rock in a 10 per cent aqueous solution of sodium ethylenedinitrilo-tetraacetate at pH 8.2. In addition to albite crystals, the insoluble residue contained a few quartz grains, carbonaceous matter, euhedral pyrite crystals, and a mixed layer clay mineral. No albite crystals were observed in a pale yellow (10YR6/2) fine- to medium-grained limestone from the same locality.

MORPHOLOGY AND OPTICAL CRYSTALLOGRAPHY

Crystal morphology. The albite occurs as euhedral crystals, tabular on (010) as shown in Figure 2, with {001}, {110}, {$\bar{1}$10}, {$\bar{1}$30}, {130}, and {$\bar{2}$01} commonly well developed. The luster of the crystal faces is considerably dulled by minute indentations of the calcite grains in the matrix and the development of vicinal planes. A channel or groove on {010} and parallel to {$\bar{1}$10} formed by a reentrant of (130) faces is designated by the arrow in Figure 2. This channel has been noted in several studies of albite from sedimentary carbonate rocks by Rose (1865), Lacroix (1897), Füchtbauer (1948), Schöner (1960), and Donnelly (1967). The dimen-

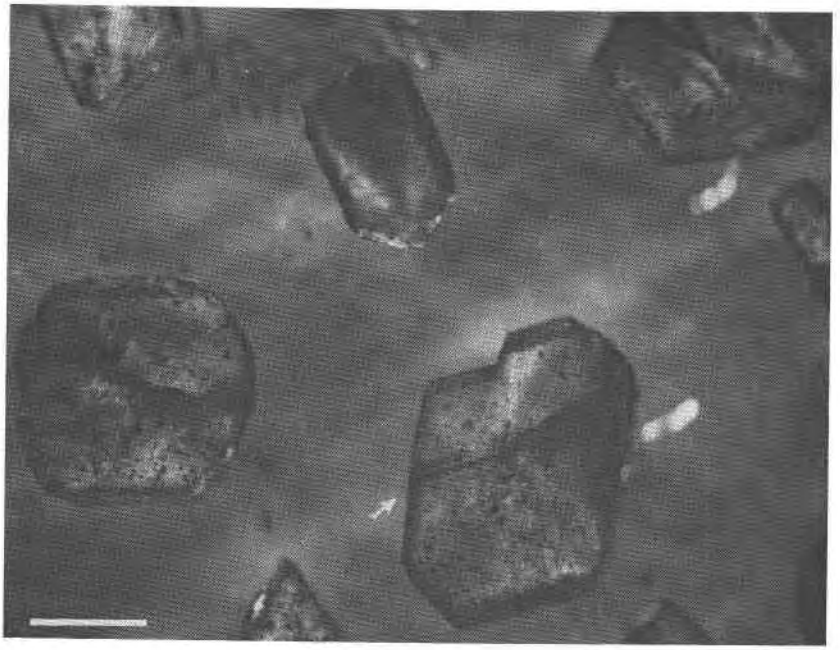

FIG. 2. Photomicrograph of Rhodian albite crystals separated from limestone by EDTA. Channel on (010) parallel to {$\bar{1}$10} visible in three largest crystals. Hourglass structure (dark) visible in crystal at top center of photograph. (crossed polars). White line in lower left represents 0.5 mm.

sions of the largest crystals studied were 1.75 mm along *a*, 0.3 mm along *b*, and 1.5 mm along *c*. The crystals stand out conspicuously on the light gray (N7) weathered outcrop surface. Von Foullon (1891) reported that the largest dimensions of albites collected from the same locality were 3, 0.5, 2.5 mm along *a*, *b*, and *c* respectively.

Twinning. The Rhodian albites are twinned after the Albite law as contact twins on (010) (Fig. 3a) and after the X-Carlsbad law as penetration twins (Figs. 3d, 3e, and 3f), each consisting of *two* individuals. Both twin types are found in the same thin section. Inasmuch as there is some confusion in the literature on twinning in authigenic feldspars, evidence supporting this identification is given in detail below.

Measurements of optical orientation and interfacial angles were obtained with a four-axis universal stage. The interfacial angles were used to independently verify that (010) is a composition surface or part of a compsition surface. Optical orientation data obtained on approximately 50 crystals are summarized below as Köhler angles (Köhler, 1942; Fisher, 1968):

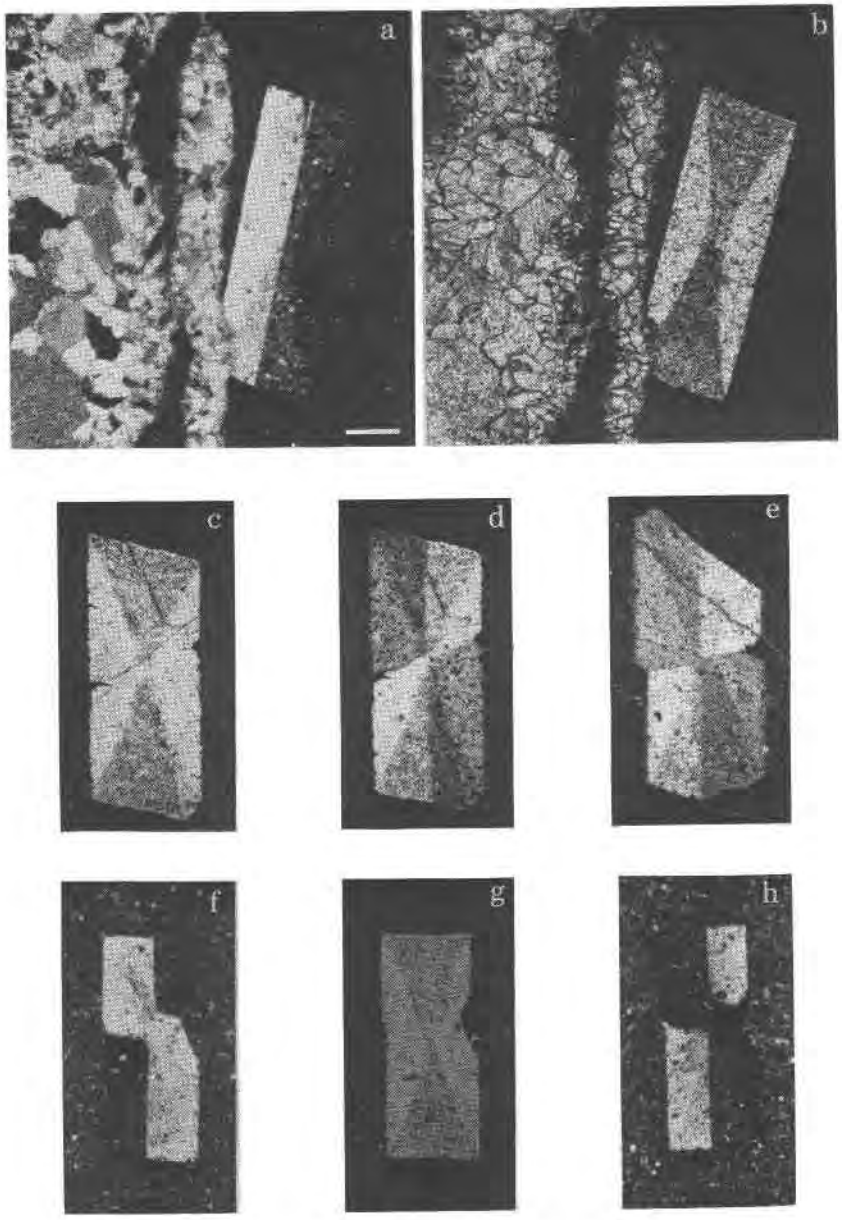

FIG. 3. Photomicrographs of albite crystals in thin section (b, c and g-plane polarized light; a, d, e, f, and h-crossed polars). Crystals are elongated parallel to {010}. Hourglass structure of calcite, quartz, and carbonaceous inclusions visible in all sections. Coarse calcite vein cuts albite and matrix in Figs. a, b, and e. Figures f, g, and h show a penetration twin in different extinction positions and in plane light. White line in lower right of Figure 3a represents 0.25 mm for all photomicrographs.

	XX'	YY'	ZZ'	AA'	BB'
Contact twins	178±1	146.5±1	33±1	83±1	85±1
Penetration twins	177.5±1	147.5±1	33±1	82±1	84±4

These results are compared in Figure 4 with the Köhler angles for other feldspar twin laws, and indicate that the Rhodian albites are either twinned after the Albite law, the X-Carlsbad law, or both. The Rhodian albites are slightly disordered (Tables 1 and 2), but this has a negligible effect on identification of the twin laws from the Köhler angles (compare data for An_{10} in Fisher's Table 1 where the optic angle is 82°).

Fisher (1968) notes that Köhler angles alone may not be sufficient to

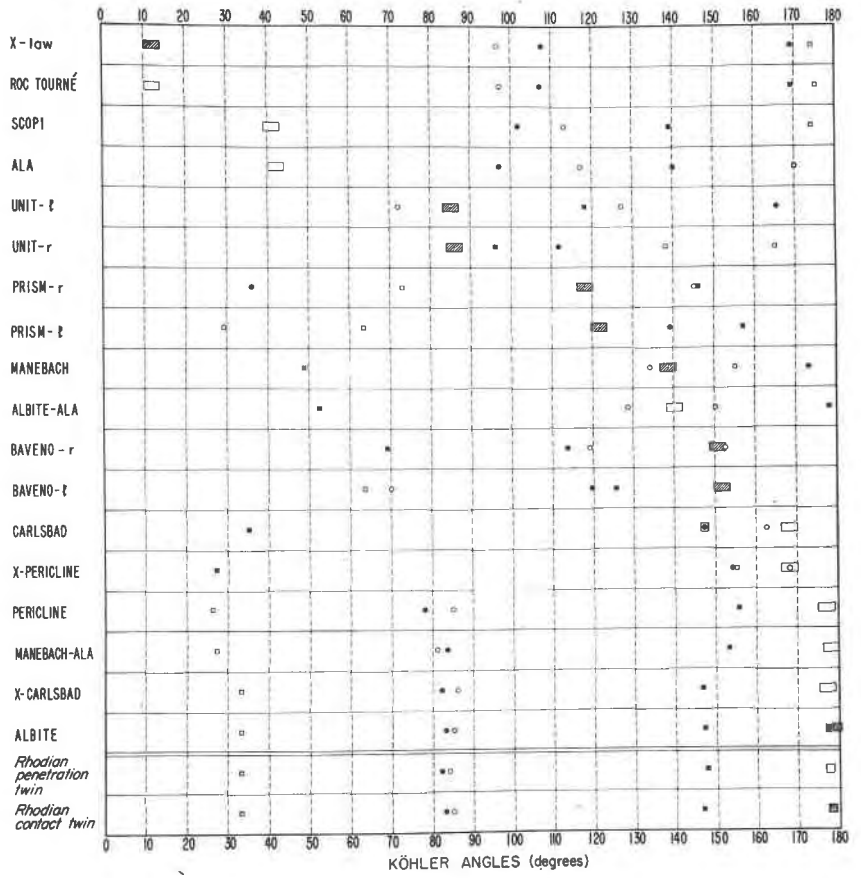

FIG. 4. Köhler angles for twins of low albite (An-content=0, Or-content=0) based on data of Fisher (1968, Table 1). Open and solid squares denote ZZ' and YY', respectively. Open and solid circles denote BB' and AA', respectively. Rectangles denote XX'; width of rectangle denotes uncertainties in all the angular values. Open rectangles refer to parallel and complex twin laws; shaded rectangles identify the "normal" twin laws.

identify feldspar twins, and in some instances it is necessary to determine the location of a twin axis on the stereographic projection. The contact twin data yield a "normal" twin projection (Turner, 1947), and the penetration twins give projections that are characteristic of "parallel" or "complex" twin laws, hence it is concluded that the contact twins represent the Albite law and the penetration twins represent the X-Carlsbad law. Other evidence indicates that the Rhodian ablites are growth twins, and thus it appears that both reflection twins[1] (Albite) and rotation twins (X-Carlsbad) developed in the same authigenic environment.

Thin sections of the penetration twins from Rhodes show two, three (Figs. 3f and 3h), or four (Figs. 3d and 3e) optically distinguishable sectors—excluding the effects produced by inclusions. However, all of the crystals studied consisted of only two individuals yielding one set of Köhler angles no matter which two adjacent sectors were compared. Similar albites are described in the literature, and are somewhat loosely referred to as 'fourling' twins. Distinguishing between twoling and fourling twins is more than a matter of definitions, inasmuch as many authors have treated 'fourling twin', 'Roc Tourné twin', and 'authigenic feldspar' as essentially equivalent terms. This has resulted in misleading and conflicting descriptions of twin laws in albites, some of which are discussed below. In the following discussion we restrict our use of the term 'fourling' to crystals of four individuals that intersect in a line, where each of the four individuals shows a different optical orientation when the crystal is sectioned at a large angle to the line. This restriction on fourling twins requires that a feldspar contain at least two twin elements, yielding two sets of Köhler angles.

Twinned albite crystals similar in morphology to the X-Carlsbad penetration twins from Rhodes were first described in detail by Rose (1865, Figs, 1, la, and 2) from Roc Tourné in Savoie, France. Rose noted that the crystals obeyed a twin law which had not been described previously for albite crystals. Lacroix (1897, Fig. 15, 20, and 21) later reproduced the same drawings of Rose and referred to them as the *Type I* Roc Tourné crystals. Based on his own study of several hundred albites from 'Roc Tourné,' Lacroix described the Type I crystals as penetration twins after the Albite and 'Roc Tourné' laws. Of critical importance here is the fact that Lacroix (p. 164) does not describe the Roc Tourné law as a single complex twin law representing a combination of the Albite and Carlsbad operations—as the Roc Tourné law is *presently* defined (Burri, 1967). The Roc Tourné laws of Lacroix and Burri are entirely different twin operations, although both are rotational twins. Neither

[1] The present authors base their discussion on Friedel's convention of using crystallographic elements of the direct lattice only as twin elements. Hence, in this paper a pseudomerohedral reflection twin is defined only by a twin plane, and a rotation twin is defined only by an axis: where the composition surface of a reflection twin is exactly planar and parallel to the twin plane, and the composition surface of a rotation twin can have any shape or orientation in the crystal (Friedel, 1926, pp. 438–439).

Turner (1947), Fisher (1968), and others refer to all feldspar reflection twins (for example the Albite law) as rotational operations by using elements of reciprocal space, while retaining the direct lattice for rotation twins. This convention is convenient for universal stage work but it is not the same as Friedel's, although both yield topologically equivalent results. This "axis-only" convention also does not permit a distinction to be made between reflection and rotation twins. We prefer to retain this distinction in that it is frequently a criterion used in evaluating genetic aspects of twinning (for example, Cahn, 1954).

Rose nor Lacroix described the Type I crystals as fourling twins; however, *if* Lacroix's description of the twin operations is correct, they *are* fourlings and should show different optical orientations in each of four sectors. Unfortunately Rose (1865) and Lacroix (1897) reported no petrographic microscope observations in their studies.

Füchtbauer (1948) described authigenic albites from Germany having a twin composition surface (or surfaces) subparallel to (100) and (010) similar to the penetration twins in Figure 3 of the present paper and the Type I crystals from Roc Tourné. He concluded that these feldspars were not twinned on the Roc Tourné law (as defined by Burri), but on the 'X-Carlsbad law' *in addition* to the Albite law. Füchtbauer's description is similar to that given by Lacroix and it appears that Füchtbauer's 'X-Carlsbad law' and Lacroix's 'Roc Tourné' law are the same, but neither follow the definition given by Burri *et al.* (1967). Füchtbauer noted only two extinction positions where four are needed to be consistent with two twin operations. His observations, however, are consistent with the present results which show the X-Carlsbad complex law alone is sufficient to describe similar twinning in the Rhodian and Cretan albites.

Donnelly (1967) also recognized that authigenic albites from the Paradox Basin, although similar in many respects to the albites from Roc Tourné, were not twinned on the Albite-Carlsbad complex law (Roc Tourné law of Burri). He described the crystals as penetration twins of the Albite law and proposed a new name, Paradox twin, for them. As can be seen in Figure 4, the X-Carlsbad law could be mistaken easily for a penetration twin of the Albite law.

As noted above, Rose (1865) and Lacroix (1897) did not refer to the Type I crystals as fourling twins. The crystals referred to as fourlings are the Type II albites from Roc Tourné. Rose begins his description of them in the following way:

> . . . Two such twinned crystals (Rose, Fig. 2) are joined into double twins such that the twinning axis for the new group is parallel to the composition plane which is the M face (010), and the twin axis is normal to the crystal main axis, as shown in Fig. 3. These crystals are twinned after the Carlsbad operation with pronounced P-plane (001), cleavage.

If the "main axis" is taken to be the *c*-axis, then the above twin operation is the Albite-Carlsbad complex law (Roc Tourné law of Burri, *et al.*, 1967).

Lacroix (1897, p. 166) describes this same crystal as a "macle triple suivant la loi de l'albite du Roc Tourné et de Carlsbad." Results of the previous discussion would suggest that Figure 3 of Rose illustrates an unusual fourling twin that is a combination of two X-Carlsbad penetration twins related by still another Albite-Carlsbad complex law operation. It is not, however, the "fourling" actually described by Rose. He continues (p. 463):

> . . . . But a peculiar thing is observed in these crystals. Those crystals that lie in the inner part of the complex are much thinner than the outer ones, and very often are completely absent as in Fig. 4 and 4a. As a result, the group then consists of 4 individuals, each of the four representing only half of the true ones. . .

This twin of "4 individuals" appears to be a true fourling in the sense that it should have four optically distinct parts which intersect in a line formed by the intersection of (010) and (100). It differs from the crystal shown in Figure 3e of this paper in which only two optical orientations can be distinguished, although there are four optical sectors intersecting at a point.

Inclusions and hourglass structure. The crystals are translucent dark gray due to numerous calcite, quartz, and carbonaceous inclusions. Thin sections (Fig. 3) and observations with the binocular microscope (Fig. 2)

show that the inclusions are confined to a volume in the center of the crystal and are distributed uniformly about the composition plane (010). The silicate portion of the crystal enclosing the inclusions has the same optical properties and chemical composition as the albite in the clearer portions of the crystal. The surface bounding the inclusion-rich and inclusion-poor volumes is best described as a hyperboloid of two sheets:

$$\frac{y^2}{f^2} - \frac{z^2}{g^2} - \frac{x^2}{e^2} = 1$$

as shown schematically in Figure 5 where $x \perp (100)$, $y \perp (010)$, and $z \perp (001)$. The geometry of the surface in Figure 5 was determined by mounting several of the albite crystals in orientations parallel to (100), (010), and (001) in a cold-setting epoxy resin. The crystals were then ground down gradually parallel to these orientatins. At various stages during grinding the crystals were viewed in transmitted light under a polarizing microscope and sketched. Figure 5 is a reconstruction of these sketches. All the crystals studied were either Albite or X-Carlsbad twins. The distribution of inclusions appears to be independent of the twin law.

The magnitudes of e, f, and g are related as $f \ll g \ll e$. Hyperbolic sections at constant x or z are both distinguishable, but sections subparallel to (100) are by far the most prominent in thin section (Fig. 3), giving rise to what is commonly called an hourglass structure. The relative magnitude e is so much larger than f and g that the surface appears to be nearly cylindrical, which accounts for the observation that most of the Rhodian albites sectioned subparallel to (100) yield an hourglass structure. Hyperbolic sections such as Figure 3b are not sections through an hourglass-shaped surface which is more accurately described as a hyperboloid of one sheet. However, no other petrographic hourglass structures such as in chiastolite (Weinschenk, 1912, pp. 196 and 298), chloritoid (Halferdahl, 1961, p. 90), and augite (Preston, 1966, p. 1228) are known to be hyperboloids of one sheet or conic surfaces, hence, a change in terminology is not warranted.

Spencer (1925) and Papastamatiou (1955, Fig. 1–2) noted that carbonaceous inclusions are often zonally arranged parallel to crystal faces in authigenic albites, and Füchtbauer (1948) sketched several crystals with inclusions located along twin boundaries. Several hourglass-type structures in feldspars are recorded in the literature. Iddings (1888) and others have described granophyric intergrowths of quartz distributed in an hourglass pattern in alkali feldspar megacrysts from volcanic rocks. Chaisson (1950, p. 542) reported an hourglass zone characterized by triclinic optics in an adularia crystal in which no significant differences in chemical composition were detected between the outer (monoclinic) and triclinic zones. Dickson and Sabine (1967) recently described an hourglass pattern of euhedral plagioclase inclusions in large euhedral barium-rich K-feldspars from quartz monzonites in southern California. The barium is distributed in alternating (oscillatory)

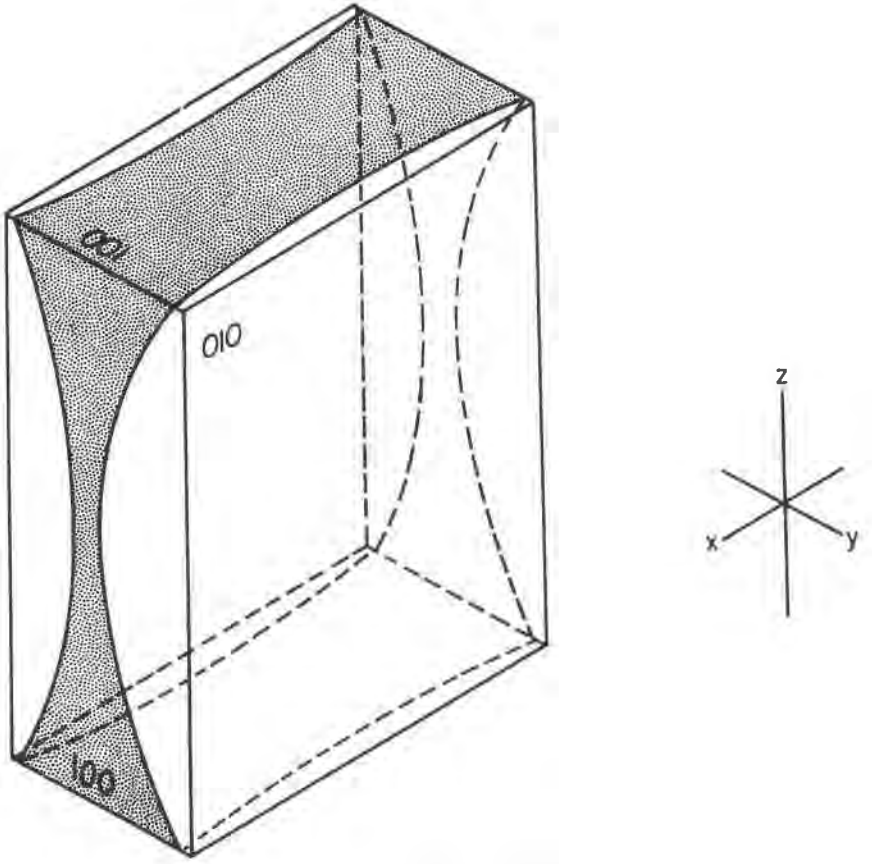

FIG. 5. Distribution of inclusions.

zones that parallel existing crystal faces, but this chemical zoning is apparently unrelated to the hourglass structure. To our knowledge, however, hourglass structure of carbonate and carbonaceous inclusions has not been described previously in feldspars or other authigenic minerals.

Optical parameters. Refractive indices of the albites were determined with an uncertainty of ± 0.001 by the immersion method at 22°C in sodium light. The refractive indices of the immersion oils were determined with an Abbé refractometer before and after each measurement. The accuracy of the data was determined by using the same methods to measure the refractive indices of a standard quartz specimen from Arkansas (Frondel and Hurlbut, 1955) kindly supplied by Professor C. Frondel.

The refractive indices α' and β' were measured on (010), and γ' was measured on (001). The same values were also obtained for these orientations on a spindle stage. Füchtbauer

(1948) found that the difference between measurements by the immersion method and values determined by the universal stage is less than 0.0005, which is within the precision of the present measurements. Hence, the results in Table 1 may be regarded as the principal refractive indices of the albites within the stated uncertainty.

The mean value of the refractive indices of the Rhodian albite is 1.5323 which compares with 1.5330 for Amelia low-albite (Doman, *et al.*, 1965), 1.5327 for Ramona albite (Emmons, 1953) and 1.5334 for metamorphic albite from the Tiburon peninsula, California (Crawford, 1966) each of which analyzed for less than 0.1 percent CaO and 0.25 percent K_2O. Assuming these Ca- and K-contents do not represent analyses of inclusions in the samples, the albites contain less than 0.5 percent $CaAl_2Si_2O_8$ and 1.5 percent $KAlSi_3O_8$ in solution. Comparing the data with the determinative curves summarized by Doman, *et al.* (1965, p. 734), Van der Plas (1966, p. 81) and Marfunin (1962, pp. 194 and 200), it is also concluded that the Rhodian albite contains less than 0.5 percent $CaAl_2Si_2O_8$ in solution. This composition also agrees with the mean refractive index (1.5323) for pure Na-feldspar calculated from Chayes' (1952) equations. The X-ray data discussed below and electron-probe microanalyses also confirm that the albites are nearly pure $NaAlSi_3O_8$.

The sign and magnitude of the optic axial angle ($2V$) were derived from the refractive indices and measured directly on a Universal Stage

TABLE 1a. OPTICAL PARAMETERS OF AUTHIGENIC ALBITES

Locality	Reference	n_α	n_β	n_γ	$\bar{n}$	$2V_\gamma$ meas.	$2V_\gamma$ calc.
Rhodes	(1)	1.528 ±.001	1.532 ±.001	1.537 ±.001	1.5323	81.0 ±2.0	83.7
Ravdoukha, Crete	(1)	1.529 ±.001	1.532 ±.001	1.536 ±.001	1.5323	—	81.9
Zweisimmen, Switzerland	(2)	1.529 ±.001	1.534 ±.001	1.540 ±.001	1.5343	85.0 ± .8	84.9
St. Maurice, Switzerland	(2)	1.529 ±.001	1.534 ±.001	1.539 ±.001	1.5340	88.5 ± .4	90.15
Bellefonte, Pennsylvania	(3)	1.529 ±.003	1.532 ±.003	1.539 ±.003	1.5333	70.0 ±5.0	66.6
Göttingen, Germany	(6)	1.528	1.532	1.536	1.5320	90.0 ±5.0	90.0

TABLE 1b. OPTICAL PARAMETERS OF LOW-ALBITES FROM PEGMATITES AND LOW-GRADE METAMORPHIC ROCKS

Locality	Reference	n_α	n_β	n_γ	$\bar{n}$	$2V_\gamma$ meas.	$2V_\gamma$ calc.
Amelia, Virginia	(4, no. 3)	1.5286	1.5325	1.5385	1.5332	78.1	77.9
Amelia, Virginia	(4, no. 5)	1.530	1.534	1.540	1.5347	—	78.6
Amelia, Virginia	(12)	1.5292	1.5328	1.5392	1.5337	81.8	73.9
Amelia, Virginia	(4, no. 7)	1.529	1.533	1.539	1.5337	79.0	78.6
Amelia, Virginia	(5)	1.5284 ±.0005	1.5320 ±.0005	1.5386 ±.0005	1.5330	—	73.1
Amelia, Virginia	(7)	1.5292 ±.0003	1.5331 ±.0003	1.5393 ±.0003	1.5338	—	76.5
Ramona, California	(8)	1.528	1.532	1.538	1.5327	75.0 80.5	78.55
Ramona, California	(9)	1.5286 ±.0003	1.5326	1.5388	1.5333	77.2 ±0.8	—
Kitani, Japan	(10)	1.530	1.534	1.540	1.5347	77.0	78.6
Tiburon, California	(11)	1.5290	1.5335	1.5395	1.5334	77.0 ±1.0	81.9
Kodarma, India	(12)	1.5285	1.5326	1.5389	1.5333	79.0	77.9
Preferred values for $NaAlSi_3O_8$	(13)	1.5274	1.5314	1.5379	1.5322	—	76.4

(1) This study
(2) Füchtbauer (1948)
(3) Honess and Jeffries (1940)
(4) Deer, *et al.* (1963 p. 110)
(5) Doman, *et al.* (1965)
(6) Baskin (1956)
(7) Viola (1907), refractometer
(8) Emmons (1953)
(9) Smith (1960)
(10) Miyakawa (1964)
(11) Crawford (1966)
(12) Spencer (1937)
(13) Chayes (1952)

(orthoscopic determination). These are compared with previously measured and calculated values in Table 1 and with curves showing the variation of optic angle with composition (Smith, 1958, 1960; Marfunin, 1962; Rankin, 1967) in Figure 6. Füchtbauer (1948, 1956) and Schöner

(1960) have noted that the optic angles of authigenic albites are significantly higher than for low albites from other geological environments. The present results are in agreement with their observations. Given that these albites are virtually pure $NaAlSi_3O_8$, the values of the optic angle shown in Figure 6 suggest that the Al/Si-distribution in these albites is not as ordered as in albites from pegmatites and metamorphic rocks. Honess and Jeffries' (1940) data for authigenic albite from Pennsylvania do not support this conclusion, but their results have a higher uncertainty than the other data in Table 1, and both their measured and calculated values of optic angles appear to be anomalously low.

The scatter in the values of refractive indices and the measured and calculated optic angle values for Amelia and Ramona albites is rather unsettling in view of the stated precision of the measurements—some measurements being made on the same specimen by two different investigators. Until optical standards such as "standard" low albite can be established and circulated among various investigators, any conclu-

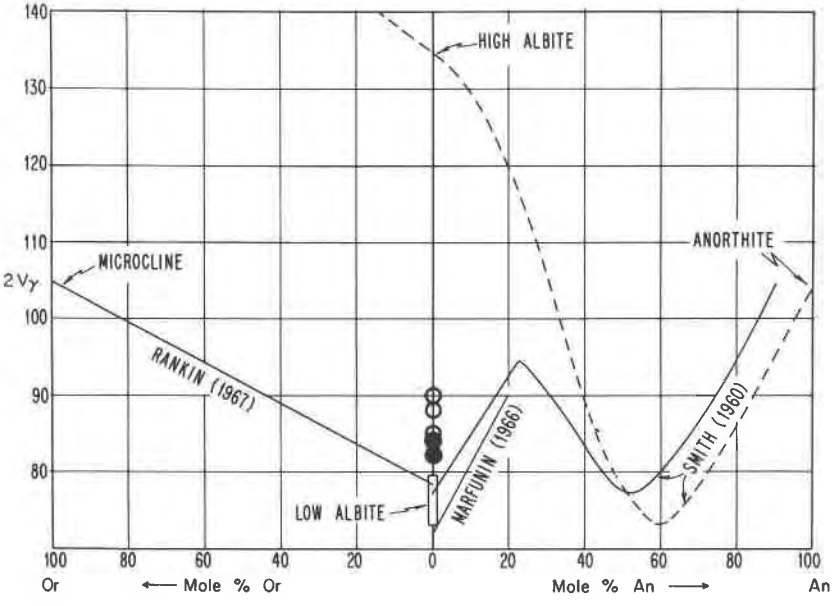

FIG. 6. Optic axial angle of alkali and plagioclase feldspars as a function of composition. Open rectangle denotes range of pegmatitic and metamorphic low-albites. Solid circles denote present data, open circles denote data of Baskin and Füchtbauer. Data for high-temperature plagioclase from Smith (1958); see also recent compilation by Burri, *et al.* (1967, Plate XII and Part 4).

sions on composition or Al-Si distribution in authigenic feldspars derived from optical data must be regarded as tentative.

X-Ray Crystallography

Experimental method. Lattice parameters of the albite crystals and the limestone matrix were determined by least-squares analysis of X-ray diffractometer data using the digital computer program of Burnham (1962). Each sample for diffraction analysis was mixed with the internal standard and deposited on a glass slide using collodion as a binder to give a permanent powder mount. A Philips wide-range X-ray goniometer (model 42201) with Ni-filtered copper radiation was used to obtain diffraction data. Three forward and two reverse scans were made at 0.25° 2θ min^{-1} in the range 20° to 60° 2θ with a chart speed of one inch per minute.

The refined lattice parameters given in Tables 2 and 4 are referred to semiconductor grade silicon (99.999% Si, <0.003 ppm B) as an internal standard. This silicon was provided by W. A. Atkinson, Department of Geological Sciences, Harvard University, and is the same material used in Waldbaum's (1966) study of alkali feldspars. Parrish's (1960) value for the lattice parameter (5.43054 ± 0.00017 Å at 25°C) was assigned to this material, and the X-ray wavelengths used in both the present calculations and the I.U.Cr. project $K_{\alpha 1}$, 1.54051; $K_{\beta 2}$, 1.54433; $K_{\beta 1}$, 1.39217 (Rieck, 1962).

Albites. The lattice parameters for the Rhodian albite in Table 2 do not differ appreciably from previous determinations of low-albites from non-sedimentary environments. These results, however, are not in agreement with the data of Baskin (1956) which indicate anomalously low cell dimensions for authigenic albites from other localities. We subsequently analyzed two other authigenic albites—both of which occur in dolostone—one from Ravdoukha, Crete (35.530°N, 23.865°E) collected by Waldbaum, and another specimen from Crete kindly provided by Professor J. N. Papastamatiou[1], University of Athens. The data in Table 2 indicate that these albites have essentially the same lattice parameters as the Rhodian albite. The K-contents of the Rhodian and Cretan albites are 0 ± 1.5 percent $KAlSi_3O_8$ as calculated from the microcline—low albite determinative data of Waldbaum (1966) and Orville (1967).

The difference between Baskin's lattice parameters and the present results are not outside the limits of precision of either set of data, but if real, they may indicate as yet unknown differences between properties and genetic histories of authigenic and other albites.

The lattice parameters plotted in Figures 7 and 8 indicate that the

[1] Papastamatiou did not specify the exact locality of this material, but it is thought that it is from the Liopetro locality noted in his 1955 paper. Albites from these two Cretan localities differ considerably in morphology and other growth features. They occur in medium-gray (N4 to N5) micritic dolostone, and as noted for the Rhodian albites, both the albites and matrix are cut by later generations of calcite veins (see also Cayeux, 1903). Optical data are given in Table 1.

TABLE 2. LATTICE PARAMETERS OF NATURAL AND SYNTHETIC $NaAlSi_3O_8$

Feldspar	Ref.	a	b	c	α	β	γ	V	α^*	γ^*	$d_{1\bar{3}1}$-d_{131}
Authigenic albite											
Rhodes	(1)	8.1380 .0014	12.7881 .0013	7.1571 .0008	94.229 .013	116.605 .009	87.807 .013	664.14 .20	86.367	90.337	0.1059
Ravdoukha, Crete	(1)	8.1365 .0026	12.7850 .0018	7.1560 .0012	94.227 .018	116.597 .014	87.789 .026	663.81 .31	86.378	90.358	0.1049
Liopetro, Crete	(1)	8.1345 .0019	12.7809 .0015	7.1561 .0008	94.206 .014	116.581 .012	87.818 .016	663.55 .26	86.387	90.337	0.1052
Gelbhorndecke, Switz.	(2)	8.125 .032	12.757 .051	7.149 .029	94.267 .170	116.700 .170	87.817 .170	660.14	86.321	90.300	0.1081
Gelbhorndecke Switz.	(2)	8.117 .032	12.749 .051	7.142 .029	94.350 .170	116.633 .170	87.783 .170	658.75	86.244	90.301	0.1105
Valentine Fm., Pa.	(2)	8.110	12.803	7.140	94.150	116.633	87.717	660.94	86.500	90.467	0.0976
Lowville Fm., Pa.	(2)	8.124	12.815	7.132	94.417	116.550	87.617	662.21	86.300	90.483	0.1063
Göttingen, Germany	(2)	8.129	12.786	7.173	93.733	116.583	88.867	665.28	86.333	89.367	0.1312
Non-authigenic low albite											
Amelia, Virginia (26°C)	(3)	8.138 .002	12.786 .003	7.163 .002	94.265 .027	116.592 .023	87.720 .023	664.64 .21	86.373	90.423	0.1035
Amelia, Virginia	(4)	8.1439 .0031	12.7879 .0027	7.1611 .0019	94.261 .026	116.582 .018	87.671 .022	665.08 .39	86.399	90.475	0.1011
Amelia, Virginia	(5)	8.1414 .0016	12.7836 .0020	7.1571 .0011	94.233 .016	116.592 .012	87.680 .015	664.25 .24	86.426	90.478	0.1001
Fused-NaCl-exchanged Amelia	(5)	8.1359 .0031	12.7844 .0049	7.1573 .0014	94.245 .022	116.568 .014	87.689 .027	663.99 .38	86.408	90.464	0.1011

TABLE 2. (*Continued*)

Feldspar	Ref.	a	b	c	α	β	γ	V	α^*	γ^*	$d_{1\bar{3}1}$-d_{131}
Kodarma, India	(9)	8.1353 .0005	12.7883 .0005	7.1542 .0005	94.226 .017	116.520 .017	87.708 .017	664.15	86.420	90.455	0.1011
Ramona, California	(6)	8.138	12.789	7.156	94.333	116.567	87.650	664.21	86.329	90.463	0.1036
Hugo, S. Dakota	(7)	8.1378 .0012	12.7817 .0019	7.1572 .0008	94.244 .018	116.619 .011	87.695 .016	663.70 .12	86.407	90.454	0.1013
High albite (analbite) Hydrothermal synthetic	(3)	8.160 .005	12.870 .007	7.106 .005	93.545 .027	116.363 .060	90.188 .008	666.98 .40	85.950	88.030	0.1845
Hydrothermal synthetic	(8)	8.160 .003	12.871 .002	7.110 .002	93.542 .035	116.362 .027	90.235 .032	667.4 .3	85.929	87.979	0.1866
Hydrothermal synthetic	(7)	8.1506 .0024	12.8616 .0020	7.1151 .0010	93.650 .019	116.451 .020	89.985 .016	666.11 .18	85.930	88.198	0.1802
Heated Amelia albite	(4)	8.1650 0.0023	12.8727 .0020	7.1115 .0014	93.455 .027	116.442 .014	90.263 .031	667.63 .30	86.010	87.985	0.1838
Heated Amelia albite	(6)	8.149	12.880	7.106	93.367	116.300	90.283	667.08	86.103	88.017	0.1801
Heated Amelia albite	(5)	8.1627 .0020	12.8729 .0016	7.1141 .0010	93.545 .019	116.460 .011	90.131 .023	667.57 .25	85.974	88.086	0.1820

(1) This study
(2) Baskin (1956)
(3) Stewart and von Limbach (1967)
(4) Smith (1956)
(5) Waldbaum (1966)
(6) Ferguson, *et al.* (1958)
(7) Orville (1967)
(8) Stewart and von Limbach (1967) based on data of Donnay and Donnay (1952)
(9) Cole, *et al.* (1951)

Values of a, b, c, and ($d_{1\bar{3}1}$-d_{131}) in Å; α, β, γ, α^*, and γ^* in degrees; V (cell volume) in Å^3. Uncertainties (least-squares standard errors) are tabulated under each direct lattice parameter. Uncertainties of reciprocal angles are approximately the same as for the direct angles.

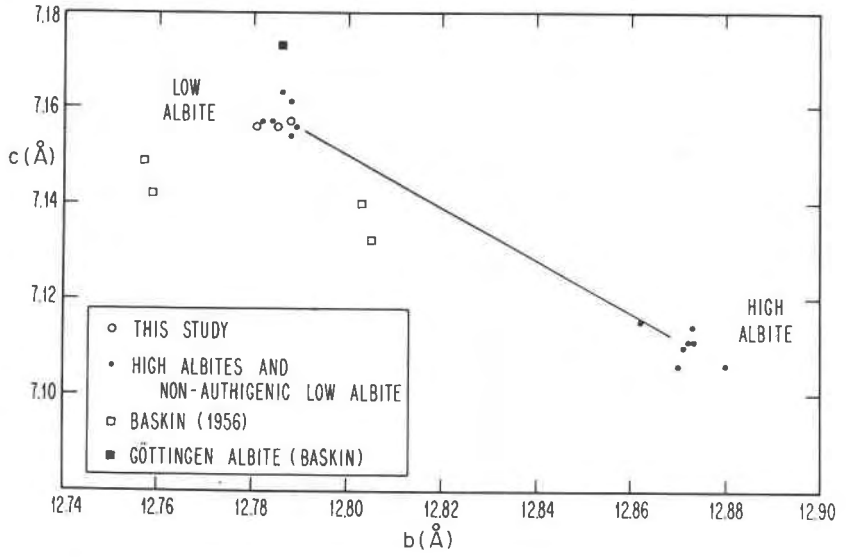

FIG. 7. Cell dimensions of albites. The line between high albite and low albite represents different states of Al-Si order in the *b*–*c* quadrilateral as determined in previous studies.

Rhodian and Cretan albites are "maximum" low albites with respect to *b* and *c*, but the relatively low values of α^* and γ^* (Table 2) and corresponding high values of $(d_{1\bar{3}1}\text{-}d_{131})$ suggest that more Al/Si-disorder may exist among the four tetrahedral sites of the authigenic albites. These results are in agreement with values of the optic angle derived from optical measurements, and are similar in this respect to the results of Reynolds (1963) and to Baskin's observations on authigenic K-feldspars and the Göttingen albite (Tables 1 and 2).

It should not be inferred from these results, however, that the Cretan and Rhodian albites crystallized at higher temperatures than albites from other geological environments or that maximum Al/Si-order is not the most stable configuration at low-temperatures. Factors other than temperature are known to influence Al/Si-ordering, but the kinetics and mechanism of ordering are as yet not well understood. MacKenzie (1957) demonstrated that Al/Si-ordering in albite is extremely sluggish at low-temperatures even when ordering is allowed to take place in the presence of pure water which acts as an efficient catalyst when compared with ordering in the dry state. In applying kinetic data to authigenic feldspars, one can assume that the original crystals grew as highly disordered phases which progressively approached a more stable state with time.

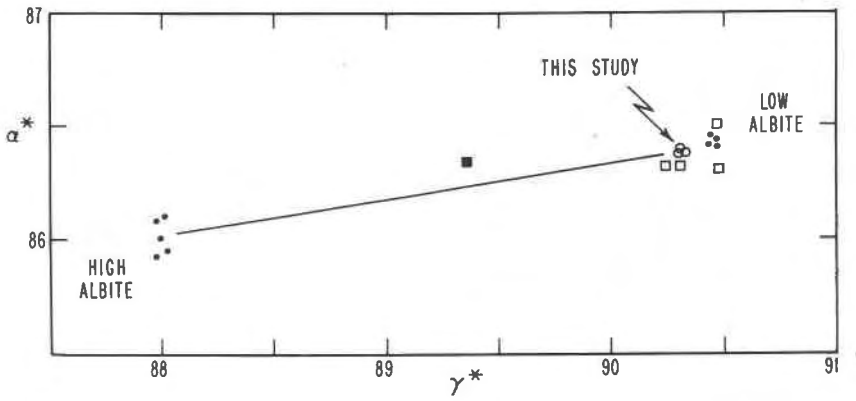

FIG. 8. Reciprocal lattice angles α^* and γ^* of high and low albites in Table 2 and Fig. 7. The line between high albite and low albite represents different states of Al-Si order in the α^*-γ^* quadrilateral as determined in previous studies.

McConnell and McKie's (1960) analysis of Mackenzie's data indicate that the time required to approach a completely ordered state in the range 25° to 100°C is on the order of 10^{16} to 10^{11} years, however, Martin (1967) has recently shown that highly ordered albite will crystallize at 200° within several weeks in the presence of excess alkali. These two conflicting sets of data alone suggest that more experimental data on the kinetics and mechanism of feldspar growth and ordering are needed before a meaningful genetic interpretation can be made from crystallographic data.

Matrix. Lattice parameters of the limestone matrix of the Rhodian albite given in Table 3 are somewhat lower than the preferred values for pure $CaCO_3$ given by Graf (1961). This is probably due to small amounts of Mg or other elements in the structure. Cathodo-luminescent properties of this rock indicate the presence of manganese, but the work of Medlin (1963) suggests that the Mn-content is on the order of 1000 ppm, which is equivalent to a decrease of 0.0002 Å in a. Assuming magnesium to be the only element present in amounts sufficient to cause detectable changes in a or c, we calculate a $MgCO_3$-content of 0.9 ± 1.0 mole percent from the following equations relating mole fraction $MgCO_3$ to a and c of synthetic magnesian calcites:

$$N(MgCO_3) = 13.8170 - 2.7712a$$

$$N(MgCO_3) = -10.0298 + 1.7427c - 0.067688c^2$$

TABLE 3. LATTICE PARAMETERS AND CELL VOLUMES OF CARBONATE MATRIX FROM ROCKS CONTAINING AUTHIGENIC ALBITES AND OF OTHER CALCITE AND DOLOMITE SPECIMENS

Material	Reference	a	c	V(Å^3)
Rhodian limestone matrix	(1)	4.9840 ± .0003	17.0392 ± .0019	366.56 ± .05
Calcite (preferred values)	(3)	4.9899	17.064	367.90
Ravdoukha, Crete dolostone matrix (fresh)	(1)	4.8106 ± .0005	16.0122 ± .0020	320.91 ± .06
Ravdoukha, Crete dolostone matrix (weathered)	(1)	4.8101 ± .0007	16.0130 ± .0026	320.86 ± .08
Liopetro, Crete dolostone matrix acid-leached)	(1)	4.8083 ± .0004	16.0056 ± .0017	320.47 ± .05
Dolomite, Binnatal, Switzerland (H.U. 10974)	(1)	4.8085 ± .0003	16.0177 ± .0014	320.74 ± .04
Dolomite, Tharandt, Germany (H.U. 10971)	(1)	4.8073 ± .0005	15.9933 ± .0021	320.09 ± .06
Dolomite, Lee, Massachusetts (cation-ordered)	(2)	4.8083	16.024	320.84
Dolomite, Serra das Eguas, Brazil (cation-ordered)	(2)	4.8098	16.028	321.12
Dolomite, Gabbs, Nevada (cation-ordered)	(2)	4.8083	16.031	320.98
Dolomite, preferred values (cation-ordered)	(3)	4.8079	16.010	320.50
Dolomite, synthetic (cation-disordered).	(2)	4.8050	16.061	321.14

(1) This study
(2) Goldsmith, *et al.* (1961)
(3) Graf (1961)

derived from the crystallographic data of Goldsmith, Graf, and Heard (1961) and Graf's (1961) preferred value for pure $CaCO_3$.

Lattice parameters of the Cretan dolomites also given in Table 3 indicate that the dolomites are highly ordered, and in fact appear to be more highly ordered than the preferred values given by Graf (1961). One pos-

sible explanation for these high values of a and low values of c is that systematic errors were introduced by the assignment of an incorrect absolute value to the cell edge of the silicon internal standard. However, one usually finds that the cell volume and all cell dimensions are either increased or decreased by this type of error, which is not the case with the data in Table 3. As a further check for systematic errors we determined the lattice parameters of two coarsely crystalline dolomites from Alpine vein deposits (Binnatal and Tharandt), and obtained values of a and c which bracket Graf's preferred values of 4.8079 and 16.010 Å. The (10.1), (10.4), and (00.3) "order" reflections of the Cretan dolomites are as sharp and intense as the same reflections of the Binnatal and Tharandt dolomites; similarly no significant differences were observed in the intensities and d-values of the (00.6) and (00.12) basal reflections. These results are additional indications that the Cretan dolomites are highly ordered, though it was not possible to determine any differences between the amount of cation or mixed-layer disorder in the Cretan dolomites and the most highly ordered dolomites studied by Graf and coworkers.

Summary and Discussion

General. The petrographic and crystallographic properties of albites from the islands of Rhodes and Crete are summarized below:

1. The crystals are growth twins with tabular euhedral shapes, and show no evidence of a detrital feldspar core. They are twinned as contact twins according to the Albite law and penetration twins after the X-Carlsbad law.

2. The albites were crystallized and developed twinning before the development of fractures and the formation of stylolites in the rock.

3. Their lattice parameters do not differ significantly from previously studied low albites from nonsedimentary environments, as is suggested by the data of Baskin (1956). The lattice parameters and optic axial angles indicate that their tetrahedral Al/Si-distribution is highly ordered, but not as ordered as low albites from pegmatites.

4. The crystals contain numerous calcite, quartz, and opaque carbonaceous inclusions which are distributed in the center of the crystals in the shape of an hourglass when viewed normal to (010). The hourglass is ubiquitous in the Rhodian albites and was found in a small percentage of the Cretan albites. Inclusions in the Cretan albites are usually found in the outer portions of the crystals parallel to the growth faces. The carbonate inclusions in the Rhodian crystals and the carbonate phase of the matrix have the same bulk composition and trace element content as

indicated by X-ray diffraction and cathodo-luminescence. The Cretan albites which are surrounded by a highly-ordered dolomite matrix contain dolomite inclusions.

The characteristic inclusions, morphology, twinning, and development of inclusion-hourglass structure indicate a crystallization environment considerably different from that of igneous and metamorphic feldspars. The present results support the conclusions of previous studies that these albites formed *in situ* during diagenesis of a carbonate sediment, and were not introduced later by hydrothermal or metasomatic fluids. Moreover, the data provide additional factors to be taken into account in developing a physico-chemical model for the nucleation and growth of authigenic albites.

Carbonate matrix. Daly (1917), Baskin (1956), and Carrozi (1960) suggested that the common association of authigenic albite with dolomite may have genetic significance. The properties of the Rhodian albites (limestone matrix) are sufficiently similar to albites occuring in dolostones that the presence of magnesium in the matrix can no longer be regarded as an essential indicator of the crystallization histories or physical properties of authigenic feldspars.

Inclusion-hourglass structure. The presence of inclusion-hourglass structure in authigenic albites provides a much clearer picture of their growth history. There is no petrographic evidence to suggest that the inclusions formed after growth of the albite, hence, in the terminology of Zerfoss and Slawson (1956) these are *primary* inclusions. The fact that similar inclusion-hourglass patterns are found in andalusite and chloritoid suggests that the nucleation and growth mechanisms for silicates during diagenesis do not differ appreciably from the mechanisms operating during higher grades of metamorphism. The close relationship of the hourglass to crystal morphology also tends to rule out the possibility that the albite crystals originated by recrystallization of an earlier authigenic mineral or amorphous aluminosilicate gel.

The interrelations between twinning and hourglass structures are not well understood inasmuch as few minerals are known to contain more than one of these features. The hourglass pattern in the Rhodian albites does not appear to depend on the form taken by the twin law since the hourglass exists in both contact and penetration twins (Fig. 3). In some sections the hourglass can be seen to converge to a point in the center of the crystal, suggesting that both the incorporation of included material and the development of twinning occurred at the very early stages of crystal growth.

Some writers (Becke, 1892; Harker, 1932, p. 42–43) have interpreted hourglass patterns of inclusions in minerals as evidence that on some faces particles were incorporated into the crystal and on others they were swept aside or pushed ahead as the crystal grew. Very little experimental evidence at either the temperature conditions of metamorphism or diagenesis exists to confirm this view except for the studies of Buckley (1934) and A. E. Corté.[1]

Corté (1963) studied the behavior of large (0.2 to 2.0 mm) particles of glass, calcite, quartz, rutile, shale, and mica at a water-ice interface during crystallization. He noted that at growth velocities less than 0.5 mm/hr all particles are *pushed* by the interface regardless of size, shape, or composition, but at higher velocities some particles are incorporated into the crystal, and at sufficiently high velocities (>10 mm/hr) none of the particles are pushed (see also Buckley, 1934, p. 250). Corté found that large particles were trapped at lower velocities. The order of the particle types trapped in the ice in order of increasing growth velocity was: glass, calcite, rutile, quartz, shale, and mica—depending on the (previously measured) relative surface energies of ice, particle, and water. In the Rhodian albites the inclusions are located along the most rapidly growing crystal faces (with the width of the hourglass zone delineating the size of the faces at the time of growth), hence, the present petrographic observations on the quartz and calcite inclusions are at least consistent with Corté's data and the mechanism proposed by Becke (1892). The carbonaceous inclusions were probably not solid at the time of crystal growth, and may have originated at the growth surface by adsorption and coalescence of organic molecules (Buckley, 1934), although evidence from other occurrences suggest that ultimate incorporation of carbonaceous material is a growth-rate controlled process.

The uniform shape of the hourglass, the uniform size of the inclusions, and homogeneous distribution of inclusions suggests further that the Rhodian albites grew at a relatively constant rate. This contrasts markedly with the erratic growth history of the Cretan albites (Papastamatiou, 1955) and Raipura albites (Spencer, 1925) which are characterized by oscillatory zones of carbonaceous inclusions.

ACKNOWLEDGEMENTS

This research was supported by National Science Foundation Grant GA-571 and the International Business Machines Corporation donation of the Harvard Computing Center. We thank Professors C. Frondel, R. Siever, and J. B. Thompson, Jr. for their suggestions on improving the manuscript. Its contents has also benefited from discussions with Prof

[1] Work done at the U. S. Army Cold Regions Research Engineering Laboratory, Hannover, N. H., in 1963 (Report 105).

J. D. H. Donnay, Johns Hopkins University; L. S. Hollister, University California at Los Angeles; and D. E. Anderson, University of Illinois; and Mr. R. Bideaux, Harvard University. Professor D. J. Fisher, University of Chicago, kindly provided a copy of his manuscript on albite twinning in advance of publication.

References

Baskin, Y. (1956) A study of authigenic feldspars. *J. Geol.*, **64,** 132–155.

Becke, F. (1892) Ueber chiastolith. *Tschermak's. Mineral. Petrogr. Mitt.*, **13,** 256–257.

Buckley, H. E. (1934) The oriented inclusion of impurities in crystals. *Z. Kristallogr.*, **88,** 248–255.

Burnham, C. W. (1962) Lattice constant refinement. *Carnegie Inst. Wash. Year Book*, **61,** 132–135.

Burri, C., R. L. Parker, E. Wenk and H. R. Wenk (1967) *Die optische Orientierung der Plagioklase.* Birkhauser Verlag, Basel, 334 pp.

Cahn, R. W. (1954) Twinned crystals. *Adv. Phys.*, **3,** 363–445.

Carrozi, A. V. (1960) *Microscopic Sedimentary Petrography.* John Wiley and Sons, N. Y., 485 pp.

Cayeux, M. L. (1903) Sur la presence de cristaux macroscopiques d'albite dans les dolomites du Trias de la Crete. *C. R. Acad. Sci. Paris*, **136,** 1703–1704.

Chaisson, U. (1950) The optics of triclinic adularia. *J. Geol.*, **58,** 537–547.

Chayes, F. (1952) Relations between composition and indices in natural plagioclase. *Amer. J. Sci.*, Bowen Vol., 85–105.

Cole, W. F., H. Sorum, and W. H. Taylor (1951) The structure of the plagioclase felspars. *Acta Crystallogr.*, **4,** 20–29.

Crawford, M. L. (1966) Optical properties of metamorphic albite. *Amer. Mineral.*, **51,** 523–524.

Daly, R. A. (1917) Low-temperature formation of alkaline feldspars in limestone. *Proc. U. S. Nat. Acad. Sci.*, **3,** 659–665.

Deer, W. A., R. A. Howie and J. Zussman (1963) *Rock Forming Minerals. Vol. 4: Framework silicates.* Longmans, Green and Co. Ltd., London, 435 pp.

Dickson, F. W., and C. Sabine (1967) Barium-zoned large K-feldspars in quartz monzonites of eastern and southeastern California. (abstr.). *Geol. Soc. Amer. Ann. Meet.*, Santa Barbara, p. 33.

Doman, R. C., C. G. Cinnamon and S. W. Bailey (1965) Structural discontinuities in the plagioclase feldspar series. *Amer. Mineral.*, **50,** 724–740.

Donnelly, T. W. (1967) Kinetic considerations in the genesis of growth twinning. *Amer. Mineral.*, **52,** 1–12.

Emmons, R. C. (1953) Selected petrogenetic relationships of plagioclase. *Geol. Soc. Amer. Mem.*, **52,** 142 pp.

Ferguson, R. B., R. J. Traill and W. H. Taylor (1958) The crystal structures of low-temperature and high-temperature albites. *Acta Crystallogr.*, **11,** 331–348.

Fisher, D. J. (1968) Cleavelandite and the signs of the optic directions. *Amer. Mineral.*, **53,** 1568–1578.

Friedel, G. (1926) *Leçons de Crystallographie.* Berger-Levrault, Paris, 602 pp.

Frondel, C., and C. S. Hulrbut, Jr. (1955) Determination of the atomic weight of silicon by physical measurements on quartz. *J. Phys. Chem.*, **23,** 1215–1219.

Füchtbauer, H. (1948) Einige Beobachtungen an authigenen Albiten. *Schweiz. Mineral. Petrogr. Mitt.*, **28,** 709–716.

——— (1950) Die nicht karbonatischen Bestandteile des göttinger Muschelkalkes mit

besonderer Berucksichtigung der Mineralneubildungen. *Heidelberger Beitr. Mineral. Petrogr.*, **2,** 235–254.

——— (1956) Zur Entstehung und Optik authigener Feldspäte. *Neues Jahrb. Mineral. Monatsh.*, **1,** 9–23.

GOLDSMITH, J. R., D. L. GRAF AND H. C. HEARD (1961) Lattice constants of the Ca-Mg carbonates. *Amer. Mineral.*, **46,** 453–457.

GRAF, D. L. (1961) Crystallographic tables for the rhombohedral carbonates. *Amer. Mineral.*, **46,** 1283–1316.

HALFERDAHL, L. B. (1961) Chloritoid: its composition, X-ray and optical properties, stability and occurrence. *J. Petrology*, **2,** 49–135.

HARKER, A. (1932) *Metamorphism.* Methuen and Co., London, 362 pp.

HONESS, A. P., AND C. D. JEFFRIES (1940) Authigenic albite from the Lowville limestone at Bellefonte, Pennsylvania. *J. Sed. Petrology*, **10,** 12–18.

IDDINGS, J. P. (1888) Obsidian Cliff, Yellowstone National Park. *U. S. Geol. Surv. Ann. Rep.* **7 (1886–1887)**, 249–295.

KÖHLER, A. (1942) Die Abhängigkeit der Plagioklasoptik vom vorangegangenen Wärmeverhalten. *Tschermak's Mineral. Petrogr. Mitt.*, **53,** 24–49.

LACROIX, A. (1897) *Mineralogie de la France et de ses Colonies* **2,** 158–169.

MACKENZIE, W. S. (1957) The crystalline modifications of $NaAlSi_3O_8$. *Amer. J. Sci.*, **255,** 481–516.

MARFUNIN, A. S. (1962) *The Feldspars-Phase Relations, Optical Properties, and Geological Distribution.* Akad. Nauk SSSR, Trudy Inst. Geol. Rudnykh Mestor., Petrogr., Mineral., Geokhim. [Transl. Israel Prog. Sci. Trans. Jerusalem, 317 pp. (1966)].

MARTIN, R. F. (1967) The synthesis of low albite. (abstr.) *Trans. Amer. Geophys. Union*, **48,** 225.

MCCONNELL, J. D. C., AND D. MCKIE (1960) The kinetics of the ordering process in triclinic $NaAlSi_3O_8$. *Mineral. Mag.*, **32,** 436–454.

MEDLIN, W. L. (1963) Emission centers in thermoluminescent calcite, dolomite, magnesite, aragonite, and anhydrite. *J. Opt. Soc. Amer.*, **53,** 1276–1285.

MIYAKAWA, K. (1964) A peculiar porphyroblastic albite schist from Nichinan-cho, Tottori Prefecture, southwest Japan. *J. Earth Sci., Nagoya Univ.*, **12,** 1–16.

ORVILLE, P. M. (1967) Unit-cell parameters of the microcline-low albite and the sanidine-high albite solid solution series. *Amer. Mineral.*, **52,** 55–86.

PAPASTAMATIOU, J. N. (1955) Sur la presence et la genese de cristaux d'albite dans quelques roches carbonateés de l'isle de Crete. *Delt. Hellenik. Geol. Etair.*, **2,** 87–97.

PARRISH, W. (1960) Results of the I. U. Cr. precision lattice parameter project. *Acta Crystallogr.*, **13,** 838–850.

PRESTON, J. (1966) An unusual hourglass structure in augite. *Amer. Mineral.*, **51,** 1227–1233.

RANKIN, D. W. (1967) Axial angle determinations in Orville's microcline-low albite solid solution series. *Amer. Mineral.*, **52,** 414–417.

REYNOLDS, R. C. (1963) Potassium-rubidium ratios and polymorphism in illites and microclines from the clay size fraction of Proterozoic carbonate rocks. *Geochim. Cosmochim. Acta*, **27,** 1097–1112.

RIECK, G. D. (1962) Tables relating to the production, wavelengths, and intensities of X-rays. In *International Tables for X-Ray Crystallography.* Kynoch Press, Birmingham **3,** 59–72.

ROSE, G. (1865) Über die Krystallform des Albits von dem Roc-Tourné und von Bonhomme in Savoyen und des Albits in allgemeinen. *Pogg. Ann. Phys. Chem.*, **125,** 457–468.

SCHÖNER, H. (1960) Über die Verteilung und Neubildung der nichtkarbonatischen Mineralkomponenten der Oberkreide aus der Umgebung von Hannover. *Heidelberger Beitr. Mineral. Petrogr.*, **7**, 76–103.

SMITH, J. V. (1956) The powder patterns and lattice parameters of plagioclase felspars. I. The soda-rich plagioclases. *Mineral. Mag.*, **31**, 47–68.

SMITH, J. R. (1958) Optical properties of heated plagioclases. *Amer. Mineral.*, **43**, 1179–1194.

——— (1960) Optical properties of low-temperature plagioclase. Appendix 3 in Hess, H. H., Stillwater Igneous Complex, Montana. *Geol. Soc. Amer. Mem.*, **80**, 191–219.

SPENCER, E. (1925) Albite and other authigenic minerals in limestone from Bengal. *Mineral. Mag.*, **20**, 365–381.

——— (1937) The potash-soda feldspars. I. Thermal stability. *Mineral. Mag.*, **24**, 453–494.

STEWART, D. B. AND D. VON LIMBACH (1967) Thermal expansion of low and high albite. *Amer. Mineral.*, **52**, 389–413.

TURNER, F. J. (1947) Determination of plagioclase with the four-axis universal stage. *Amer. Mineral.*, **32**, 389–410.

VAN DER PLAS, L. (1966) *The Identification of Detrital Feldspars*. Elsevier, Amsterdam, 305 pp.

VIOLA, C. (1907) Feldspathstudien. *Z. Kristallogr.*, **43**, 202–209.

VON FOULLON, H. B. (1891) Über Gesteine und Minerale von der Insel Rhodus. *Sitzber. Konig. Akad. Wiss. Wien. Math. Naturw. Kl.* **100C**, Abt. 1, 144–176.

WALDBAUM, D. R. (1966) *Calorimetric investigation of alkali feldspars*. Ph.D. Thesis, Harvard University, 247 pp.

WEINSCHENK, E. (1912) *Petrographic Methods*. McGraw-Hill, New York, 396 pp.

ZERFOSS, S., AND S. I. SLAWSON (1956) Origin of authigenic inclusions in synthetic crystals. *Amer. Mineral.*, **41**, 598–607.

Manuscript received, August 15, 1967; accepted for publication, June 19, 1968.